Volume 56
Number 10
4 February 2020
Pages 1451–1612

ChemComm

Chemical Communications

rsc.li/chemcomm

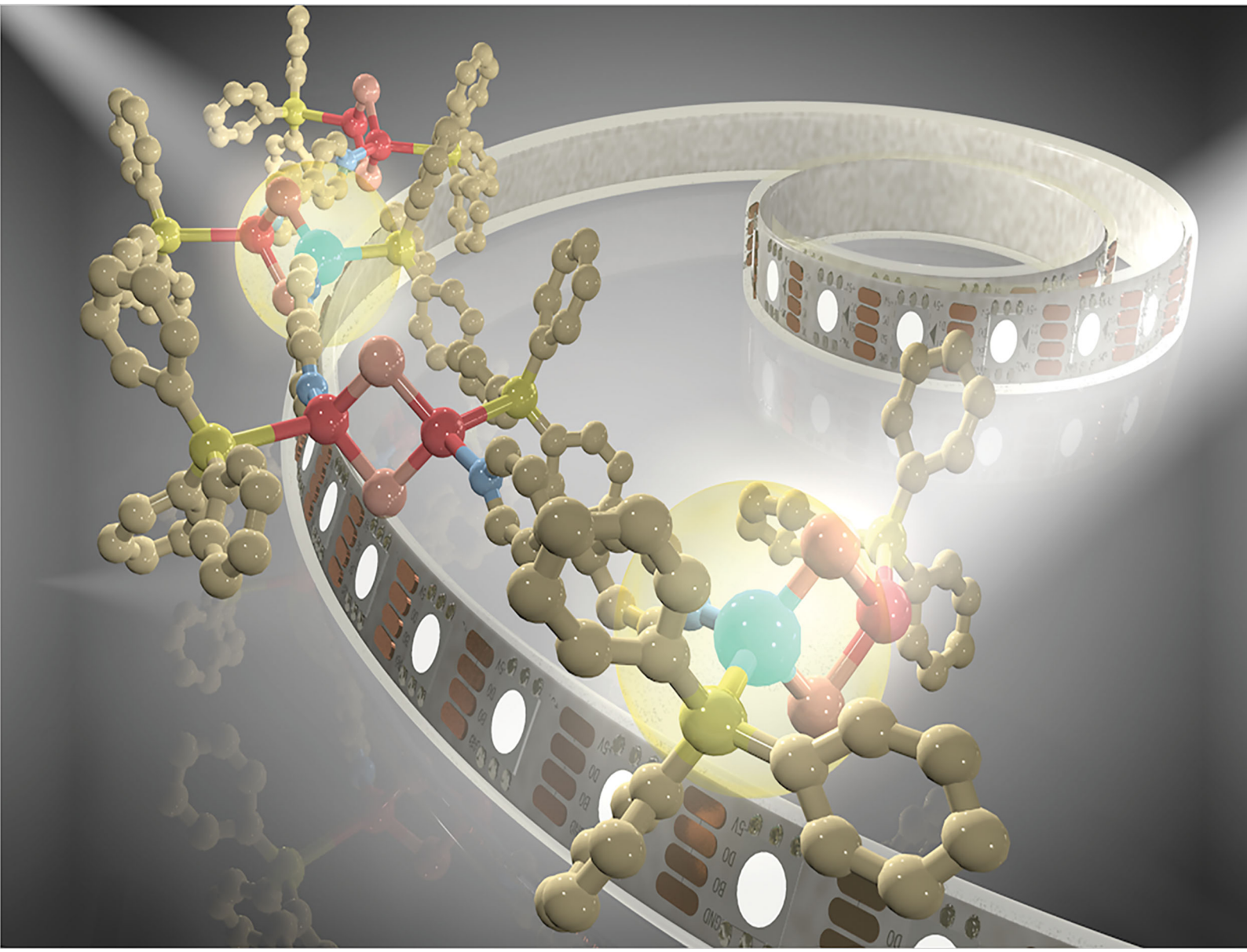

ISSN 1359-7345

ROYAL SOCIETY OF CHEMISTRY

COMMUNICATION

Wei Liu, Jing Li *et al.*

Strongly emissive white-light-emitting silver iodide based inorganic–organic hybrid structures with comparable quantum efficiency to commercial phosphors

ChemComm

COMMUNICATION

View Article Online
View Journal | View Issue

Cite this: *Chem. Commun.*, 2020, **56**, 1481

Received 28th November 2019,
Accepted 2nd January 2020

DOI: 10.1039/c9cc09260a

rsc.li/chemcomm

Strongly emissive white-light-emitting silver iodide based inorganic–organic hybrid structures with comparable quantum efficiency to commercial phosphors†

Fang Lin,[a] Wei Liu,*[a] Hao Wang[a] and Jing Li*[ab]

A series of one-dimensional silver iodide based inorganic–organic hybrid structures with tunable white light emissions have been synthesized by Cu substitution. The white-light-emitting hybrid 1D-$Ag_{2-x}Cu_xI_2L_2$ ($x < 2$, L = ligand) compounds exhibit extremely strong luminescence with internal quantum yield (IQY) as high as 95%, significantly higher than most of the previously reported direct white-light-emitting hybrid structures and comparable to the IQYs of commercial phosphors.

The replacement of traditional energy-costly incandescent bulbs with LED lamps is a critical step forward towards reducing overall electrical consumption worldwide.[1,2] Since the current white light-emitting diodes (WLEDs) are primarily single chip based, phosphors are generally needed to coat on the surface of the LED chip to generate white light.[3] This class of LEDs is termed phosphor converted (pc-) WLEDs.[4] The emission spectrum of a WLED covers the entire visible light region (400–700 nm) and is typically produced by the combination of a blue light excitable yellow-emitting phosphor with a blue LED chip.[5] The most commonly used commercial blue-excitable yellow phosphor is cerium-doped yttrium aluminum garnet (YAG:Ce), with an IQY of around 95% when excited by a blue light.[6,7] However, white light obtained from this type of WLED generally lacks the low energy emission contribution and often has an increased correlated color temperature (CCT) that is too "cold" for indoor illumination.[6,8] Moreover, nearly all of the commercial phosphors in the market today contain rare-earth elements (REEs), which brings up potential supply, cost, and environmental issues.[9,10]

Crystalline inorganic–organic hybrid materials are composed of standalone inorganic and organic moieties or modules blended at the atomic or molecular scale, and they have been extensively explored over the past several decades.[11–16] Numerous single-phase, REE free, direct white-light-emitting hybrid phosphors have been reported to date, including structures built by II–VI (Zn, Cd and S, Se) based semiconductors, 2D perovskites, *etc.*[17–23] These types of phosphors aim to overcome the above-mentioned issues, generating white light of higher quality with lower CCT values. However, their IQYs are much lower compared to those of commercial phosphors, which hinders their practical applications.

Inorganic–organic hybrid materials based on IB–VIIA binary compounds exhibit enormous structural variety.[24–26] A number of inorganic modules have been found, from discrete molecular units to infinite chains or layers. Such inorganic motifs are further connected by different kinds of organic ligands, either aliphatic or aromatic, forming zero dimensional (0D) molecular clusters to one dimensional (1D) chains, and from two dimensional (2D) sheets to three dimensional (3D) frameworks.[24,27–29] The emission profiles of nearly all of these structures are single-band type, with full width at half maximum (FWHM) of around 100 nm.[30,31] These materials display a number of advantages compared to commercial phosphors and other types of luminescent materials, such as strong luminescence, earth abundancy, REE free, facile one-step synthesis, *etc.* Based on earlier studies, ligand doping has been proven to be an effective approach in broadening the emission peak in order to achieve white light.[32,33] For other types of hybrid structures, metal doping/substitution have been reported as a useful method for optimizing the luminescence properties.[34,35] Here, we expand our work to explore the effect of metal substitution in IB–VIIA based hybrid structures.

In this paper, a series of copper(I) substituted silver(I) iodide based 1D inorganic–organic hybrid materials built on M_2I_2 rhomboid dimers have been prepared (Fig. 1). They have the general formula of 1D-$Ag_{2-x}Cu_xI_2(tpp)_2(4,4'\text{-bpy})$ ($x < 2$, tpp = triphenylphosphine, 4,4′-bpy = 4,4′-bipyridine). Pure Ag based 1D-$Ag_2I_2(tpp)_2(4,4'\text{-bpy})$ emits blue light (λ_{em} = 460 nm), while pure Cu based 1D-$Cu_2I_2(tpp)_2(4,4'\text{-bpy})$ emits yellow light (λ_{em} = 550 nm) under UV light irradiation.[36,37] Bright white light has

[a] *Hoffmann Institute of Advanced Materials, Shenzhen Polytechnic, 7098 Liuxian Blvd, Nanshan District, Shenzhen, 518055, China. E-mail: weiliu2018@szpt.edu.cn*

[b] *Department of Chemistry and Chemical Biology, Rutgers University, 123 Bevier Road, Piscataway, NJ, 08854, USA. E-mail: jingli@rutgers.edu*

† Electronic supplementary information (ESI) available: Experimental details, PXRD patterns, TGA data, DFT calculation results, elemental analysis results, ICP-MS results and PL spectra. See DOI: 10.1039/c9cc09260a

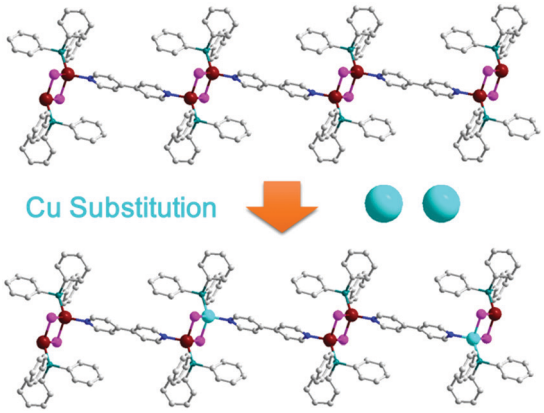

Fig. 1 Illustration of the copper substitution in 1D-$Ag_2I_2(tpp)_2(4,4'\text{-bpy})$. (red ball) Ag; (pink ball) I; (light blue ball) Cu; (gray ball) C; (dark blue ball) N; (green ball) P.

been observed for all Cu substituted samples, with internal quantum yield (IQY) ranging from 78% to 95%. As far as we are aware, this value is the highest among all direct white-light-emitting hybrid structures. In addition, their emission spectra can be tuned by varying the substitution amount of Cu. The advantages of high quantum efficiency, facile synthesis and emission tunability make this type of hybrid material a promising candidate as a general lighting phosphor.

Silver(I) based hybrid structures are much less investigated compared to copper(I) based analogues.[38–45] Like Cu(I), the closed-shell d^{10} electronic configuration of Ag(I) can adopt coordinated geometries, forming a variety of inorganic modules, including clusters, chain or layers including the AgX monomeric unit, the rhomboid Ag_2X_2 dimer, the AgX staircase chains, the Ag_2X_2 helical chains, the wavelike Ag_4X_4 chains, and the hexagonal prism-shaped Ag_6X_6 cluster.[26,38,41,44,46,47] Previous studies reveal that silver halide based hybrid structures have similar structure types and photophysical properties compared to copper halide based hybrid structures.[30,48] Among different inorganic motifs for IB–VIIA semiconductor based hybrid structures, molecular cluster based structures such as rhomboid dimers generally exhibit much higher quantum yields compared to others with higher dimensionality.[49] The highly emissive dimer core can be incorporated into an extended framework to enhance the thermal stability of the resultant network structures.[50] Taking these desirable features into consideration, we deliberately selected a strongly luminescent Ag_2I_2 rhomboid dimer based hybrid compound 1D-$Ag_2I_2(tpp)_2(4,4'\text{-bpy})$ as the parent structure for the metal substitution study. In 1D-$M_2I_2(tpp)_2(4,4'\text{-bpy})$ (M = Ag or Cu), each metal ion in the rhomboid dimer motif is tetrahedrally coordinated to two iodine atoms and two organic ligands, one is tpp and the other is 4,4′-bpy. The bidentate 4,4′-bpy coordinates to the metal ions in the adjacent dimer motifs, forming a 1D extended structure.

1D-$Ag_2I_2(tpp)_2(4,4'\text{-bpy})$ (**1**), 1D-$Cu_2I_2(tpp)_2(4,4'\text{-bpy})$ (**6**) and the substituted structures 1D-$Ag_{2-x}Cu_xI_2(tpp)_2(4,4'\text{-bpy})$ (x = 0.001, 2; x = 0.005, 3; x = 0.01, 4; x = 0.02, 5) have been obtained by simply stirring the AgI, CuI, tpp and 4,4′-bpy in DMF/DCM at room temperature. As tpp was introduced in the reaction mixture, the products typically adopt rhomboid dimer based structures as the steric hindrance of tpp would prevent the formation of other inorganic modules.[49] Their phase purities have been analyzed by PXRD analysis as shown in Fig. S1 (ESI†). The PXRD patterns of all substituted samples match with the simulated pattern of 1D-$Ag_2I_2(tpp)_2(4,4'\text{-bpy})$, indicating that the substitution of Cu into the Ag hybrid does not change the parent structure. The actual substitution amounts of Cu have been determined by ICP-MS and the results have been summarized in Table S1 (ESI†). The substitution amount of Cu has been controlled to less than 1% of Ag in order to avoid the possibility of the formation of mixed phases. Thermal stability of these compounds was evaluated by thermogravimetric (TG) analysis (Fig. S2, ESI†). The decomposition temperature (T_D) of **1** was estimated to be 160 °C and the T_D of **6** is around 200 °C. The T_D for the substituted samples is almost identical to that of **1**.

DFT calculations on 1D-$Ag_2I_2(tpp)_2(4,4'\text{-bpy})$ (**1**) show that the valence band maximum (VBM) is composed primarily of the inorganic module, namely Ag 4d and I 5p atomic orbitals, while the conduction band minimum (CBM) is made up dominantly of the LUMO orbital (C 2p, N 2p and P 3p atomic orbitals) of the organic ligands (Fig. 2a). The results show that substitution of Ag to Cu would change the energy of the valence band and the band gaps. The calculated band structure of **1** has been plotted in Fig. S3 (ESI†). Optical absorption spectra for compounds **1–6** are shown in Fig. 2b. The experimental band gaps for **1** and **6** are 3.0 eV and 2.2 eV, respectively. After substitution of **1**, the experimental band gap slightly shifted to lower energies, as expected. All substituted samples exhibit a single strong absorption edge without any other absorption at the lower energy part, indicating that there is no other phase formed and the Cu ions have been substituted into the parent structure.

1 exhibits intense blue emission (λ_{em} = 460 nm) under near-UV excitation (λ_{ex} = 360 nm) with IQY as high as 86%. Its copper analogue **6**, emits intense yellow emission peaked at 550 nm, with IQY of 78% at the same excitation energy. The addition of a trace amount of CuI together with AgI in the synthesis leads to the formation of samples **2–5**. Photoluminescence measurements of the substituted structures show that their emission energies change significantly compared to that of their parent structure (Fig. 3a). The blue emission band from their parent structure still remains, while a second band emerges in the PL spectra located in the yellow light region as the effect of the substitution. The emerged yellow emission band combines with the blue emission band, forming a broader band covering the entire visible light region. Though compound **6** could be excited by blue light (450 nm), compound **1** and substituted compound (**2–5**) can only be excited by UV light as shown in their excitation spectra (Fig. S4, ESI†).

The relative intensities of the blue band and yellow band under various excitation wavelengths have been studied (Fig. S5, ESI†). The observation of their excitation-wavelength dependent emission suggests that the two emission bands are from isolated luminous centers. The time-resolved PL measurements were conducted on **4** under the excitation of 360 nm at the emission maximum of the two bands (Fig. S6, ESI†). The lifetime values

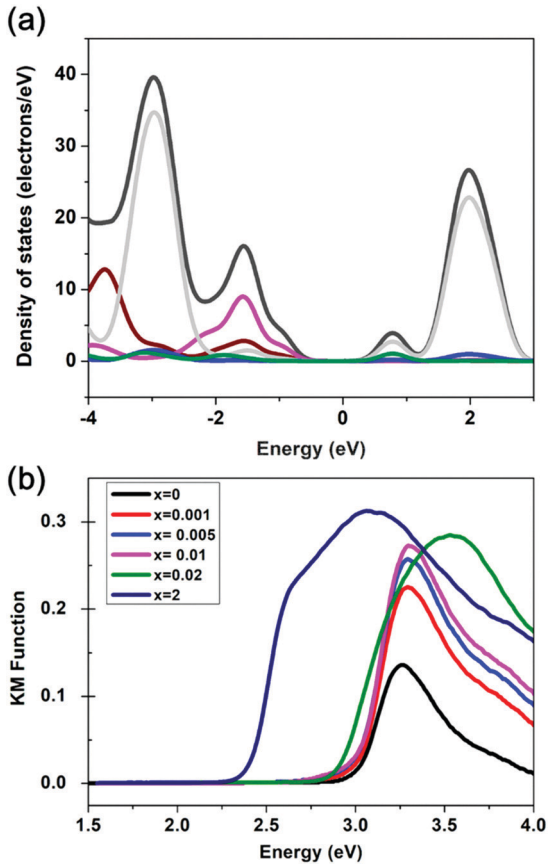

Fig. 2 (a) Calculated density of states (DOS) of **1** by the DFT method: total DOS (black); Ag 4d orbitals (dark red); I 5p orbitals (pink); C 2p orbitals (grey); N 2p orbitals (blue); P 3p orbitals (green). (b) Optical absorption spectra for compounds 1D-$Ag_{2-x}Cu_xI_2(tpp)_2(4,4'\text{-bpy})$ ($x < 2$).

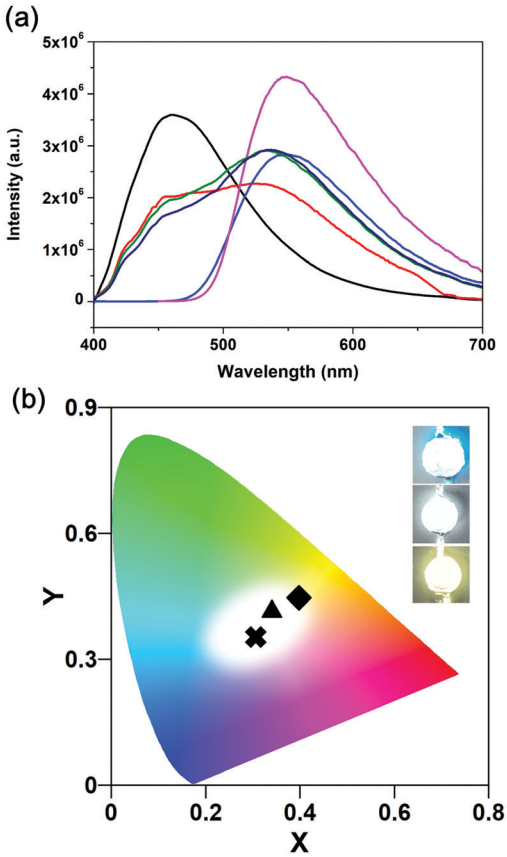

Fig. 3 (a) Photoluminescence spectra of **1** (black), **2** (red), **3** (green), **4** (navy), **5** (blue), and **6** (pink); λ_{ex} = 360 nm. (b) CIE coordinates of **2** (cross), **3** (triangle) and **4** (square). Inset: Photos of the LED bulbs coated by **2**–**4** under working conditions.

for emissions at 460 nm and 550 nm are 20.8 μs and 3.4 μs, respectively. The difference of the lifetime values illustrates their different excited states.

Compounds **2**–**4** emit white light and could be potentially useful as white-lighting-emitting lighting phosphors. Their performances as lighting phosphors were evaluated by IQY measurements, chromaticity color coordinates (CIE), Color Rendering Index (CRI) and CCT under the excitation of near-ultraviolet light (360 nm) and the results are summarized in Table 1. It is fascinating that the IQYs of the substituted structures are higher than that of their parent structure, with the highest value of 95% for compound **4**. This value is comparable to the commercial phosphors.[51] Based on our knowledge, they are among the highest IQYs for direct white-light-emitting inorganic–organic hybrid materials. The CCT values of these compounds could also be tuned, from bluish (cold) to yellowish (warm) white light (Fig. 3b). Metal doping/substitution has been widely used for the optimization of the optical properties of inorganic–organic hybrid materials, and the efficient energy transfer between the host and the doped metal ions is responsible for the enhancement of luminescence.[35,52] The cost of the raw materials of the hybrid phosphors and YAG has been summarized in Table S3 (ESI†).

Table 1 Summary of the composition and optical properties of 1D-$Ag_{2-x}Cu_xI_2(tpp)_2(4,4'\text{-bpy})$ ($x < 2$)

#	x	Bandgap (eV)	λ_{em} (nm)	IQYs (%) λ_{ex}: 360 nm	CIE	CRI	CCT (K)
1	0	3.0	460	86	0.15, 0.16	—	—
2	0.001	3.0	460, 550	90	0.33, 0.42	63	5628
3	0.005	3.0	460, 550	92	0.35, 0.43	65	5034
4	0.01	3.0	460, 550	95	0.43, 0.45	67	4578
5	0.02	2.9	460, 550	91	0.38, 0.56	—	—
6	2	2.2	550	78	0.38, 0.58	—	—

In summary, a series of copper(I) substituted silver(I) iodide inorganic–organic hybrid structures have been obtained and they exhibit strong white light emission, with IQY as high as 95%, comparable to the IQYs of commercial phosphors. The white light of these materials is tunable based on the substitution amount of Cu. This work provides another approach for the generation of white light, and may be applied to other hybrid material families.

Conflicts of interest

There are no conflicts to declare.

Notes and references

1 P. M. Pattison, J. Y. Tsao, G. C. Brainard and B. Bugbee, *Nature*, 2018, **563**, 493–500.
2 N. Armaroli and V. Balzani, *Energy Environ. Sci.*, 2011, **4**, 3193–3222.
3 Y. Wei, G. Xing, K. Liu, G. Li, P. Dang, S. Liang, M. Liu, Z. Cheng, D. Jin and J. Lin, *Light: Sci. Appl.*, 2019, **8**, 15.
4 J. H. Oh, H. Kang, Y. J. Eo, H. K. Park and Y. R. Do, *J. Mater. Chem. C*, 2015, **3**, 607–615.
5 M.-S. Wang and G.-C. Guo, *Chem. Commun.*, 2016, **52**, 13194–13204.
6 X. Huang, *Nat. Photonics*, 2014, **8**, 748–749.
7 Y. H. Kim, P. Arunkumar, S. H. Park, H. S. Yoon and W. B. Im, *Mater. Sci. Eng., B*, 2015, **193**, 4–12.
8 H. Zhu, C. C. Lin, W. Luo, S. Shu, Z. Liu, Y. Liu, J. Kong, E. Ma, Y. Cao, R.-S. Liu and X. Chen, *Nat. Commun.*, 2014, **5**, 4312.
9 B. Sprecher, I. Daigo, S. Murakami, R. Kleijn, M. Vos and G. J. Kramer, *Environ. Sci. Technol.*, 2015, **49**, 6740–6750.
10 A. Tukker, *Environ. Sci. Technol.*, 2014, **48**, 9973–9974.
11 C. R. Kagan, D. B. Mitzi and C. D. Dimitrakopoulos, *Science*, 1999, **286**, 945–947.
12 B. Saparov and D. B. Mitzi, *Chem. Rev.*, 2016, **116**, 4558–4596.
13 X. Huang and J. Li, *J. Am. Chem. Soc.*, 2007, **129**, 3157–3162.
14 D. B. Mitzi, *Progress in Inorganic Chemistry*, John Wiley & Sons, Inc., 2007, pp. 1–121, DOI: 10.1002/9780470166499.ch1.
15 X. Huang, J. Li and H. Fu, *J. Am. Chem. Soc.*, 2000, **122**, 8789–8790.
16 J. Li and R. Zhang, *Progress in Inorganic Chemistry*, John Wiley & Sons, Inc., 2011, pp. 445–504, , DOI: 10.1002/9781118148235.ch8.
17 W. Ki and J. Li, *J. Am. Chem. Soc.*, 2008, **130**, 8114–8115.
18 W. Ki, J. Li, G. Eda and M. Chhowalla, *J. Mater. Chem.*, 2010, **20**, 10676–10679.
19 L. Mao, P. Guo, M. Kepenekian, I. Hadar, C. Katan, J. Even, R. D. Schaller, C. C. Stoumpos and M. G. Kanatzidis, *J. Am. Chem. Soc.*, 2018, **140**, 13078–13088.
20 L. Mao, Y. Wu, C. C. Stoumpos, M. R. Wasielewski and M. G. Kanatzidis, *J. Am. Chem. Soc.*, 2017, **139**, 5210–5215.
21 G. Wu, C. Zhou, W. Ming, D. Han, S. Chen, D. Yang, T. Besara, J. Neu, T. Siegrist, M.-H. Du, B. Ma and A. Dong, *ACS Energy Lett.*, 2018, **3**, 1443–1449.
22 Z. Yuan, C. Zhou, Y. Tian, Y. Shu, J. Messier, J. C. Wang, L. J. van de Burgt, K. Kountouriotis, Y. Xin, E. Holt, K. Schanze, R. Clark, T. Siegrist and B. Ma, *Nat. Commun.*, 2017, **8**, 14051.
23 C. Zhou, H. Lin, H. Shi, Y. Tian, C. Pak, M. Shatruk, Y. Zhou, P. Djurovich, M.-H. Du and B. Ma, *Angew. Chem.*, 2018, **130**, 1033–1036.
24 R. Peng, M. Li and D. Li, *Coord. Chem. Rev.*, 2010, **254**, 1–18.
25 S. Shibata, K. Tsuge, Y. Sasaki, S. Ishizaka and N. Kitamura, *Inorg. Chem.*, 2015, **54**, 9733–9739.
26 W. Liu, W. P. Lustig and J. Li, *Energy Chem.*, 2019, **1**, 100008.
27 W. Liu, K. Zhu, S. J. Teat, G. Dey, Z. Shen, L. Wang, D. M. O'Carroll and J. Li, *J. Am. Chem. Soc.*, 2017, **139**, 9281–9290.
28 W. Liu, Y. Fang and J. Li, *Adv. Funct. Mater.*, 2018, **28**, 1705593.
29 Y. Fang, W. Liu, S. J. Teat, G. Dey, Z. Shen, L. An, D. Yu, L. Wang, D. M. O'Carroll and J. Li, *Adv. Funct. Mater.*, 2017, **27**, 1603444.
30 P. C. Ford, E. Cariati and J. Bourassa, *Chem. Rev.*, 1999, **99**, 3625–3648.
31 K. Tsuge, Y. Chishina, H. Hashiguchi, Y. Sasaki, M. Kato, S. Ishizaka and N. Kitamura, *Coord. Chem. Rev.*, 2016, **306**(Part 2), 636–651.
32 W. Liu, D. Banerjee, F. Lin and J. Li, *J. Mater. Chem. C*, 2019, **7**, 1484–1490.
33 X. Zhang, W. Liu, G. Z. Wei, D. Banerjee, Z. Hu and J. Li, *J. Am. Chem. Soc.*, 2014, **136**, 14230–14236.
34 M. Zhang, C. Shi, T.-K. Zhang, M. Feng, L. Chang, W.-T. Yao and S.-H. Yu, *Chem. Mater.*, 2009, **21**, 5485–5490.
35 M. Roushan, X. Zhang and J. Li, *Angew. Chem.*, 2012, **124**, 451–454.
36 R.-Z. Li, D. Li, X.-C. Huang, Z.-Y. Qi and X.-M. Chen, *Inorg. Chem. Commun.*, 2003, **6**, 1017–1019.
37 J. T. Sampanthar and J. J. Vittal, *Cryst. Eng.*, 2000, **3**, 117–133.
38 L. Chen, J. Ma, Q. Chen, R. Feng, F. Jiang and M. Hong, *Inorg. Chem. Commun.*, 2012, **15**, 208–211.
39 D. Sun, F.-J. Liu, R.-B. Huang and L.-S. Zheng, *Inorg. Chem.*, 2011, **50**, 12393–12395.
40 D. Yang, W. Xu, X. Cao, S. Zheng, J. He, Q. Ju, Z. Fang and W. Huang, *Inorg. Chem.*, 2016, **55**, 7954–7961.
41 S. Yuan, S.-S. Liu, H.-F. Lu, M.-Z. Xu and D. Sun, *Acta Crystallogr., Sect. C: Cryst. Struct. Commun.*, 2013, **69**, 216–218.
42 M. Dosen, Y. Kawada, S. Shibata, K. Tsuge, Y. Sasaki, A. Kobayashi, M. Kato, S. Ishizaka and N. Kitamura, *Inorg. Chem.*, 2019, **58**, 8419–8431.
43 A. V. Artem'ev, M. Z. Shafikov, A. Schinabeck, O. V. Antonova, A. S. Berezin, I. Y. Bagryanskaya, P. E. Plusnin and H. Yersin, *Inorg. Chem. Front.*, 2019, **6**, 3168–3176.
44 A. V. Artem'ev, M. R. Ryzhikov, A. S. Berezin, I. E. Kolesnikov, D. G. Samsonenko and I. Y. Bagryanskaya, *Inorg. Chem. Front.*, 2019, **6**, 2855–2864.
45 G. Chakkaradhari, T. Eskelinen, C. Degbe, A. Belyaev, A. S. Melnikov, E. V. Grachova, S. P. Tunik, P. Hirva and I. O. Koshevoy, *Inorg. Chem.*, 2019, **58**, 3646–3660.
46 A. M. Ortiz, P. Gómez-Sal, J. C. Flores and E. de Jesús, *Organometallics*, 2014, **33**, 600–603.
47 M. Trivedi, G. Singh, A. Kumar and N. P. Rath, *Inorg. Chim. Acta*, 2015, **438**, 255–263.
48 V. W.-W. Yam, V. K.-M. Au and S. Y.-L. Leung, *Chem. Rev.*, 2015, **115**, 7589–7728.
49 W. Liu, K. Zhu, S. J. Teat, B. J. Deibert, W. Yuan and J. Li, *J. Mater. Chem. C*, 2017, **5**, 5962–5969.
50 W. Liu, Y. Fang, G. Z. Wei, S. J. Teat, K. Xiong, Z. Hu, W. P. Lustig and J. Li, *J. Am. Chem. Soc.*, 2015, **137**, 9400–9408.
51 R. C. Ropp, in *Studies in Inorganic Chemistry*, ed. R. C. Ropp, Elsevier, 2004, vol. 21, pp. 447–614.
52 X. Fang, M. Roushan, R. Zhang, J. Peng, H. Zeng and J. Li, *Chem. Mater.*, 2012, **24**, 1710–1717.

